Available online at www.sciencedirect.com
ScienceDirect
Applied Catalysis B: Environmental 81 (2008) 88–96
APPLIED CATALYSIS B: ENVIRONMENTAL
www.elsevier.com/locate/apcatb

Effect of Pd precursor salt on the activity and stability of Pd-doped hexaaluminate catalysts for the CH_4 catalytic combustion

A. Baylet *, S. Royer, P. Marécot, J.M. Tatibouët, D. Duprez

LACCO, UMR CNRS 6503, Université de Poitiers, 40 Avenue du Recteur Pineau, 86022 Poitiers Cedex, France

Received 28 September 2007; received in revised form 29 November 2007; accepted 8 December 2007
Available online 31 January 2008

Abstract

This study reports the influence of palladium salt precursor on the catalytic activity of palladium-doped hexaaluminate catalysts for the combustion of 1 vol% CH_4 in the presence of CO_2 and H_2O as inhibitors. Thermal stability of the catalysts is evaluated in long-term catalytic test at 700 °C. The hexaaluminate supports were synthesized using two different procedures: conventional coprecipitation and solid/solid diffusion procedure. Palladium impregnation was carried out by two different routes using $Pd(NO_3)_2$ in water or $Pd(acac)_2$ in toluene as impregnation solution. It was observed that using $Pd(acac)_2$ as precursor allows to attain higher dispersion of the active phase (Pd particles size <3 nm). Compared to the catalysts obtained by impregnation of $Pd(NO_3)_2$, higher catalytic activities are then obtained. Nevertheless, a deactivation of the samples obtained using $Pd(acac)_2$ is observed. At the end of the stability test, almost similar catalytic activity is obtained whatever the palladium precursor. Reduction–reoxidation experiment showed that this deactivation is irreversible, and TEM analysis suggest that this deactivation is related to the sintering of Pd particles under reaction over samples synthesized using $Pd(acac)_2$ as precursor.

Keywords: Methane combustion; Hexaaluminate; Palladium salt effect; Activity; Thermal stability

1. Introduction

Since the beginning of the 1990s, methane catalytic combustion appears as an alternative technology to conventional thermal combustion for energy production [1]. Compared to conventional combustion process, using a catalyst allows to decrease the reaction temperature, leading to a decrease in noxious emissions of nitrogen oxides. Nevertheless, the stability of the catalysts at the temperature of work is the main problem encountered [2]. Some of the catalysts presenting promising properties for such applications are perovskites and hexaaluminates [3]. The minimum temperature necessary for the crystallization of these mixed oxides (i.e. 600 °C for the perovskites [4] and 1100 °C for the hexaaluminates [5]) makes these solids excellent candidates for reaction at high temperature, since high-thermal stability can be achieved on these solids. Nevertheless, the catalytic activity of such pure oxides samples remains low, in comparison with those obtained on conventional noble metal oxidation catalysts [6]. This was clearly observed on hexaaluminate samples for which very low activity toward methane oxidation is measured up to 700 °C. The highest catalytic activities at low and intermediate temperature were generally obtained over palladium-based catalysts, oxidized palladium catalysts generally presenting the best performances [7]. Unfortunately, conventional oxidation catalysts (generally composed of palladium and/or platinum dispersed on alumina) strongly deactivate under reaction for intermediate/high reaction temperatures (>600 °C) [6,7]. In the case of palladium-based catalysts, deactivation is attributed to two different processes: progressive reduction of the palladium oxide clusters [8]; sintering of the support and/or palladium particles [9]. As a consequence, the nature of the support, as well as the chemical state and particle size of palladium are key parameters to maintain high activity and high long-term stability. Then, many investigations carried out on the influence of the support concluded that catalytic properties and stability under reaction of Pd-based catalyst strongly depend on the nature of the support, and on the interaction that exists between the palladium particles and the support. As a matter of fact, the nature of the support, is found to strongly influence the thermal

* Corresponding author. Tel.: +33 5 49 45 35 22; fax: +33 5 49 45 34 99.
E-mail address: alexandre.baylet@etu.univ-poitiers.fr (A. Baylet).

0926-3373/$ – see front matter © 2007 Elsevier B.V. All rights reserved.
doi:10.1016/j.apcatb.2007.12.004

stability of the catalysts [10,11] especially when redox properties confer very high-oxygen mobility to the solid.

In previous work [6], hexaaluminate materials were found to present excellent stability for the methane combustion at high temperature. Indeed, the stability obtained over such catalyst was largely higher than those obtained for perovskite-type catalysts [6]. In this work, hexaaluminate samples of general formula ($La_{0.2}Sr_{0.3}Ba_{0.5}MnAl_{11}O_{19}$) were prepared using two different synthesis methods. The first way of synthesis consists in the carbonate coprecipitation [6,12–14] and the second one is an original method consisting in a solid/solid reaction at high temperature of La, Sr, Ba and Mn cations beforehand impregnated onto a porous alumina support [15]. Since literature reported differences in term of palladium particle size with the palladium precursor, and consequently on the catalytic activity [16], two ways of palladium impregnation ($Pd(NO_3)_2$ in water or $Pd(acac)_2$ in toluene) were used to prepare the catalysts. Sample activities and stabilities were measured for the oxidation of 1.0 vol% CH_4 in air containing combustion gases (CO_2 and H_2O are added to the feed due to their inhibitor effects, and to simulate exhaust gases). A reference Pd/Al_2O_3 sample was prepared for the sake of comparison.

2. Experimental

2.1. Catalyst preparation

Support synthesis procedure was fully described in a previous work [15], and will be only summarized here. Main characteristics of the support (synthesis route and support composition) are summarized in Table 1. The first synthesis route, initially proposed by Groppi et al. [12–14] consists in the simultaneous precipitation of the nitrate precursors using $NH_4(CO_3)_2$ as precipitation agent. The amounts of precursors were adjusted to obtain 5 g of solid after calcination. Nitrate precursors were first dissolved in water and heated at 60 °C. The solution containing the precursors is then slowly added to a solution containing ammonium carbonate (adjusted at pH 10) pre-heated at 60 °C, resulting in the hydroxide precipitation. At the end of the addition, the pH of the solution is verified to be comprised between 8 and 8.5. The precipitate is aged for 4 h under slow stirring. After ageing, the solid is recovered by filtration, extensive washing and dried at 120 °C. After drying, the sample is calcined at 1100 °C under flowing air (temperature ramp = 5 K min^{-1}; isothermal time = 4 h) in order to crystallize the amorphous precursor into the hexaaluminate phase. The second way of synthesis consists in the reaction of the nitrate precursors of lanthanum, strontium, barium and manganese with aluminium cations of a porous support. The use of a porous support was expected to maintain a high specific surface area in the final solid. The porous support used for the preparation is a γ-Al_2O_3 from AXENS in the form of alumina beads (diameter = 2 mm). Before use, the beads were hand crushed, and sieved to 100–200 μm. The obtained powder was calcined in airflow at 650 °C for 2 h. Then, 5 g of γ-Al_2O_3 sample was immersed in an alkaline solution of dilute NH_4OH (pH 8) heated at 60 °C. The solution containing the nitrate precursors (La, Sr, Ba and Mn) previously dissolved in water was then slowly added to the alkaline solution containing alumina under vigorous stirring. During precipitation, the pH is maintained at pH 8 by continuous NH_4OH addition. After ageing for 30 min, the solid was filtered, washed with distilled water, and dried at 120 °C over night. After drying, the sample was heated in airflow by increasing the temperature at 2 K min^{-1} up to 1100 °C and maintained at this temperature for 4 h. Samples studied in this work were named HCa when hexaaluminate support was prepared by carbonate coprecipitation or HP when the solid/solid diffusion route was used (Table 1).

Palladium impregnation was performed using two different procedures. For all the samples, the amount of palladium precursor was adjusted to obtain a theoretical metal loading of 1.0 wt% after impregnation and calcination. The palladium loading used for this work remains low in comparison with that used in many academic references (up to 10 wt%) [7,16–18]. Nevertheless, high-metal dispersions, and consequently high catalytic activities, can be obtained using this loading [15] compared to those obtained at higher metal loading [16,18]. The first impregnation route consists in a conventional aqueous impregnation procedure of the palladium nitrate (aqueous impregnation: Pd_{aq}, Table 1). The hexaaluminate sample (3 g) was first dispersed under stirring in an acidified solution (20 mL of diluted HNO_3, pH 2). A second solution containing the palladium precursor ($Pd(NO_3)_2$, Johnson Matthey, 7.63 wt% Pd) was slowly added. At the end of the addition, the water was evaporated under vacuum at 60 °C. The so-obtained powder was dried over night at 120 °C, and then calcined in airflow at 650 °C for 2 h (temperature increasing ramp = 5 K min^{-1}). The second impregnation route consists in an impregnation procedure using palladium bis-acetylacetonate in dry toluene (organic impregnation: Pd_{org}, Table 1). Palladium bis-acetylacetonate ($Pd(C_5H_7O_2)_2$), Alfa Aesar, 49.5 wt% Pd) previously dissolved in toluene was slowly added to the solution containing the support (3 g) dispersed in toluene (20 mL). At

Table 1
Synthesis procedures and nomenclature of the catalysts studied in this work

Sample	Support synthesis procedure	Support composition	Pd source
Pd/REF	Commercial γ-Al_2O_3, AXENS	Al_2O_3	$Pd(NO_3)_2$
Pd_{aq}/HCa	Carbonate precipitation	$La_{0.2}Sr_{0.3}Ba_{0.5}MnAl_{11}O_{19}$	$Pd(NO_3)_2$
Pd_{org}/HCa	ID	ID	$Pd(acac)_2$
Pd_{aq}/HP	Solid/solid diffusion, based on 100 wt% of hexaaluminate in the final oxidic compound	ID	$Pd(NO_3)_2$
Pd_{org}/HP	ID	ID	$Pd(acac)_2$

the end of the addition, the solvent was slowly evaporated under vacuum, and the obtained solid dried over night at 120 °C. Prior to use, the catalyst was calcined in airflow at 650 °C for 2 h (temperature increasing ramp = 2 K min^{-1}).

All the results obtained on the palladium-doped hexaaluminate were compared to those obtained on a conventional oxidation catalyst (Pd/Al_2O_3) prepared using the aqueous impregnation route of palladium nitrate onto γ-Al_2O_3 support (AXENS). Before impregnation, the support was calcined in airflow at 650 °C for 2 h.

2.2. Characterization

Pd quantification was performed by ICP-OES using a PerkinElmer Optima 2000 DV apparatus. Prior to the analysis, the samples were dissolved in concentrated HCl using microwave heating to ensure a complete dissolution of the samples.

BET specific surface areas were obtained by conventional N_2 adsorption at 77 K, using a Tristar instrument from MICROMERITICS. About 0.5 g of catalyst was first evacuated at 200 °C under vacuum for 6 h before N_2 adsorption.

Palladium dispersion was evaluated by means of H_2 chemisorption. Analysis was carried out on a Micromeritics AutoChemII instrument. After reduction of the sample under H_2 (350 °C for 1 h), and purge under Ar at the same temperature for 3 h, the sample was cooled down to 70 °C and maintain to this temperature in order to avoid Pd–H hydride formation. Then, H_2 pulses were injected at regular interval times (10 min). Dispersion is calculated using the following equation [19], by supposing that one hydrogen atom is adsorbed per palladium atom:

$$D\,(\%) = \frac{2P_{H_2}V_{H_2}M_{Pd}}{RTx_m m_{cata}} \quad (1)$$

With P_{H_2}, hydrogen pressure (Pa); V_{H_2}, volume adsorbed (mL); $R = 8.314$ J K^{-1} mol^{-1}; $T = 295$ K; m_{cata}, catalyst weight (g); M_{Pd} palladium molar weight (106.4 g mol^{-1}); x_m, palladium loading (wt%).

Palladium particle size is determined by using the following equation [19], supposing spherical particles:

$$d\,(\mathrm{nm}) = 6 \times 10^5 \frac{M_{Pd}}{\rho_{Pd} D S_{Pd}} \quad (2)$$

With ρ_{Pd}, palladium density (12 g cm^{-3}); D, dispersion (%); S_{Pd}, molar surface area of palladium assuming an equidistribution of the low index faces ($S = 47{,}780$ m^2 mol^{-1} for Pd metal).

2.3. Methane oxidation reaction

Catalytic activity was measured for the oxidation of 1.0 vol% CH_4. For each test, a weight of 27.5 mg of catalyst diluted in 250 mg of SiC was introduced between two quartz wool plugs in a U-shaped quartz microreactor (i.d. = 5 mm). After reactor purge under N_2, a total flow rate of 190 mL min^{-1} composed of (vol%) $1.0CH_4$–$4.0CO_2$–$4.0H_2O$–$18.2O_2$–$72.8N_2$ passed through the reactor previously stabilized at the temperature of 50 °C. Test conditions correspond to a gas hourly space velocity (GHSV) of 415,000 mL g^{-1} h^{-1}. After stabilization of the reacting mixture, the test began with a first temperature ramp (5 K min^{-1}) from 50 °C to 700 °C. At the end of the ramp, the reactor was cooled to 50 °C under reaction flow (temperature decrease ramp = −20 °C min^{-1}). Two temperature ramps were performed successively in order to evaluate the effect of the cooling under the reacting mixture, and to have access to some information about catalyst stability. Temperature was then ramped at 5 °C min^{-1} for a second time from ambient temperature up to 700 °C under the same gas mixture. At the end of the second ramp, catalyst temperature was stabilized at 700 °C and maintained at this temperature for 12 h in order to evaluate catalyst stability (stability test).

Reactants and reaction products were analyzed using a VARIAN GC3900 gas chromatograph equipped with a FID detector. A Porapak Q column (i.d. = 6 mm, $L = 0.3$ m) was used to separate the reaction products. Tests were considered valid when carbon balance (defined as the sum of non-converted CH_4 and produced CO_2 divided by the initial CH_4) was between 95% and 105%. Details concerning calculations of activation energies and relative activities can be found in Ref. [15]. Activation energies are directly extrapolated from the Arrhenius plot in the low activity range (i.e. for conversion lower than 20%).

3. Results and discussion

3.1. Physical characterization

The structural and physical properties of the two supports (HCa and HP) were presented in a previous work [15], and will be only succinctly summarized here for sake of simplicity. The specific surface of the supports HP and HCa is 7 m^2 g^{-1} and 19 m^2 g^{-1}, respectively. The HCa sample presents diffraction lines assigned to the hexagonal alumina rich hexaaluminate phase with an important contribution of the $SrAl_{12}O_{19}$ phase. Small diffraction peaks which can be assigned to α-Al_2O_3 are also observed. A similar diffractogram was obtained on the HP sample. Nevertheless, the main difference consists in higher relative intensities of the diffraction peaks attributed to the α-Al_2O_3 in this sample with respect to those obtained for the hexaaluminate diffraction lines. Because the two samples were calcined at the same temperature, this suggests a higher contamination of the HP sample by α-Al_2O_3 phase. Moreover, the smaller specific surface area obtained for the HP sample (7 m^2 g^{-1}) supports this interpretation since α-Al_2O_3 [15] generally presents a very low specific surface area.

Slight differences are observed between the theoretical amount of palladium, and the experimental one evaluated by mean of ICP (Table 2). Amounts of palladium vary then between 1.1 wt% (Pd/REF, Pd_{aq}/HCa) and 0.8 wt% (Pd_{aq}/HP 1.00). The two samples prepared from the organic impregnation route present a metal loading of 0.9 wt%.

Dispersions and palladium particle sizes are summarized in Table 2. The Pd/REF sample presents the highest dispersion

Table 2
Physical properties of the studied catalysts

Samples	S_{BET} ($m^2\ g^{-1}$)	Pd[a] (wt%)	H_2 chemisorbed ($\mu mol\ H_2\ g^{-1}$)	Dispersion[b] (%)	Pd crystallite size[c] (nm)
Pd/REF	190	1.1	5.02	67	1.4
Pd_{aq}/HCa	19.5	1.1	1.83	24	3.8
Pd_{org}/HCa	18.8	0.9	3.53	55	1.7
Pd_{aq}/HP	11.2	0.8	1.41	26	3.5
Pd_{org}/HP	8.9	0.9	2.08	34	2.7

[a] Evaluated by ICP-MS (after dissolution in H_2SO_4).
[b] Calculated supposing the adsorption of one H atom with one accessible Pd atom.
[c] Determined using equation $d(nm) = 6 \times 10^5\ (M_{Pd}/\rho_{Pd}DS)$, with M_{Pd}, palladium mass; ρ_{Pd}, palladium density (12 g cm^{-3}); D, palladium dispersion (%); S, structural factor ($4.7780.10^4\ m^2\ mol^{-1}$ for metallic palladium).

($D = 67\%$) among the solids presented here. The calculated palladium particle size, assuming cubic particles, is 1.4 nm (Table 2). No appreciable change in specific surface area can be observed after impregnation, which remains almost the same as for the support (190 $m^2\ g^{-1}$ for Pd/REF, 185 $m^2\ g^{-1}$ for REF) (Table 2). Dispersion obtained in this work over the Pd/REF sample is close to those reported in the literature for Pd/alumina samples [20].

Whatever the impregnation route, palladium impregnation onto hexaaluminate support (HCa and HP 1.00) leads to lower dispersions than that obtained for the Pd/REF sample. When palladium nitrate was used as precursor, dispersions of 24% and 26% are obtained for the Pd_{aq}/HCa and Pd_{aq}/HP samples, respectively. The corresponding mean particle sizes (3.8 and 3.5 nm, respectively) are more than 2.5 times higher than for the Pd/REF sample. The use of palladium bis-acetylacetonate ($Pd(acac)_2$) allows to increase the dispersions: 55% and 34% for Pd_{org}/HCa and Pd_{org}/HP, respectively (Table 2). Even if palladium loadings are slightly different, it is clear that the use of palladium bis-acetylacetonate as palladium precursor allows to obtain higher dispersion of the active phase. Such increase in metal dispersion was already reported in the literature using different palladium precursors. For example, Simplicio et al. [16] reported palladium dispersions varying from 2.1% (alumina was impregnated with $PdCl_2$) to 18.3% (alumina impregnated with $Pd(acac)_2$). Nevertheless, the palladium loading differs (1.0 wt% in our case, 3.0 wt% in Ref. [16]), that can explain why largely lower dispersion is reported by these authors. Similarly, Monteiro et al. [21] reported higher dispersions using palladium chloride and palladium bis-acetylacetonate as palladium source (around 50%), whereas palladium nitrate leads to lower dispersion (16%). As already observed for the REF sample, impregnation of 1 wt% Pd does not cause any drastic change in specific surface area that remains almost constant whatever the impregnation route.

3.2. Catalytic activity in methane combustion

Samples were tested in oxidation of 1.0 vol% methane under oxidizing conditions at a GHSV = 415,000 mL $g^{-1}\ h^{-1}$. 4.0 vol% of CO_2 and H_2O were added into the feed in order to simulate exhaust gases. For stable Pd_{aq} catalysts, where differences in terms of conversion between the first and the second ramp did not exceed 10%, only results obtained during the second temperature ramp are presented here, and used for activity calculations. Whereas both light-off curves are presented for Pd_{org}-based samples, since the difference between first and second temperature ramp is too important to be neglected.

Catalytic activities of the supports alone (without palladium) were already presented in Ref. [15]. Very low catalytic activities were then measured whatever the synthesis procedure used. Only a slightly higher catalytic activity was obtained over HCa due to its twice higher specific surface area.

For the palladium-doped samples studied in this work, large differences in terms of catalytic activity can be observed (Fig. 1A, results obtained during the second temperature ramp). The highest activity is obtained for the Pd/REF sample, the temperature at 15% methane conversion (T_{15}) being 425 °C. The Pd_{org}/HCa sample presents slightly lower catalytic activity, with a T_{15} equals to 523 °C (Table 3). The three other samples (Pd_{aq}/HCa, Pd_{org}/HP and Pd_{aq}/HP) present largely lower catalytic activity, with T_{15} equal to 605 °C, 645 °C and 690 °C, respectively. Based on the experimental activity measured at 600 °C (A_{600}, Table 3), the catalytic activity varies as it follows: Pd/REF > Pd_{org}/HCa ≫ Pd_{aq}/HCa > Pd_{org}/HP > Pd_{aq}/HP.

The two solids prepared using the aqueous impregnation procedure present similar palladium dispersion (Table 2). Nevertheless, a higher activity is obtained for the Pd_{aq}/HCa with respect to that obtained for the Pd_{aq}/HP (Fig. 1A). The difference between the two samples is supposed to mainly originate from the difference in palladium loading between the two samples (Table 2). For the samples prepared using the organic impregnation procedure, a higher palladium dispersion is obtained on the Pd_{org}/HCa. This can explain why this sample presents a higher catalytic activity than the Pd_{org}/HP sample.

Contrarily to what was observed for the Pd_{aq} catalysts, Pd_{org} catalysts show deactivation after the first temperature ramp (Fig. 2). The maximum of methane conversion obtained at 700 °C is lower after the second temperature ramp: 54% for Pd_{org}/HCa whereas 74% was obtained at the end of the first light-off. Similar trend was observed for Pd_{org}/HP. As mentioned above, changing the nature of the palladium precursor allows to obtain different palladium dispersions. Higher dispersions were then obtained using $Pd(acac)_2$ as palladium source instead of $Pd(NO_3)_2$. On the HCa support, the dispersion is found to increase from 24% (using palladium

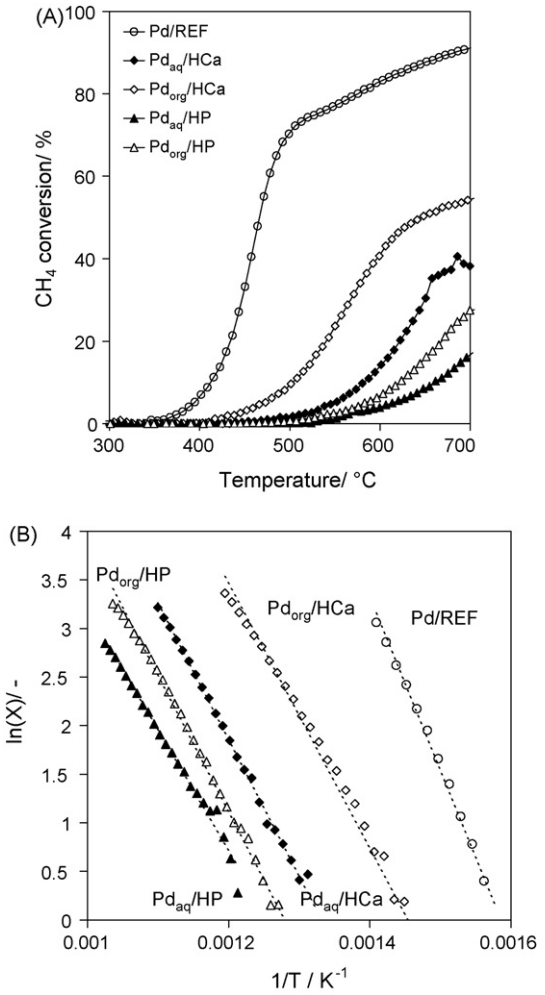

Fig. 1. Light-off curves (A) and corresponding Arrhenius plots ($X < 20\%$ of methane conversion) (B) obtained on the different samples for the oxidation of 1 vol% methane during the second temperature ramp.

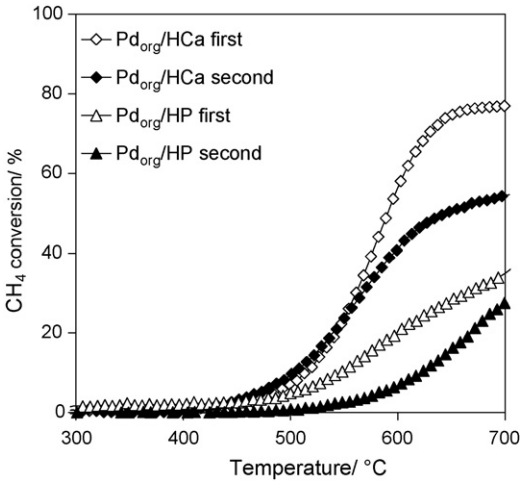

Fig. 2. Light-off curves obtained on the Pd_{org} catalysts for the oxidation of 1 vol% methane during the first and the second light-off step.

nitrate) to 55% (using palladium bis-acetylacetonate) (Table 2), consistently with the highest catalytic activity observed for the Pd_{org}/HCa sample. Then, the T_{15} decreases from 605 °C to 523 °C, and the activity at 600 °C (A_{600}, Table 3) increases from 0.18 $\mu mol_{CH_4}\ s^{-1}$ to 0.62 $\mu mol_{CH_4}\ s^{-1}$ for Pd_{aq}/HCa and Pd_{org}/HCa, respectively. Similar trend is observed for the palladium supported HP samples. The use of $Pd(acac)_2$ as palladium precursor has been studied by Lesage-Rosenberg et al. [22] who observed highly dispersed phases using this precursor. Moreover, samples prepared from organic precursors showed the highest activities for methane combustion [22], as already observed by Simplicio et al. [16]. Highest activity for CH_4 combustion and highest thermal stability is then generally obtained over sample synthesized using palladium bis-acetylacetonate ($T_{10} = 270$ °C) [16]. For comparison, catalysts synthesized from palladium chloride ($T_{10} = 378$ °C) or palladium nitrate ($T_{10} = 334$ °C) showed largely lower catalytic activity, due to lower Pd dispersion. The activities (T_{15}, Table 3) reported for our solids are largely lower than those reported by Simplicio et al. [16], which can be explained by different experimental conditions: (i) low GHSV (60,000 mL $g^{-1}\ h^{-1}$) (ii) absence of inhibitor (0.5% CH_4/2% O_2/97.5% N_2) and higher Pd loading: 3.0 wt% instead of 1.0 wt% Pd. The T_{10} reported by Jang et al. [23] over a series of 2 wt% Pd/$Sr_{1-x}La_xMnAl_{11}O_{19}$ (with $x = 0$, 0.4, 1) is found to vary between 360 °C and 450 °C. Indeed, reaction is performed using 1.0 vol% in air at a GHSV of only 70,000 mL $g^{-1}\ h^{-1}$ with no CO_2 or H_2O added to the feed. Similarly, Sekizawa et al. [24] reported T_{10} lower than 500 °C for a series of 1.44 wt% Pd over $Sr_{0.8}La_{0.2}Mn_xAl_{12-x}O_{19}$ ($x = 0$, 1) samples. Nevertheless, the GHSV used by the authors remained 8.5 times lower than that used in this work, and no inhibitor was added to the feed.

Table 3
Catalytic activity and activation energy obtained over the different samples

Samples	T_{15}[a] (°C)	E_a[b] (kJ mol^{-1})	X_{700}[c] (%)	A_{600}[d] ($\mu mol_{CH4}\ s^{-1}$)
Pd/REF	425	148	91	1.06
Pd_{aq}/HCa	605	116	79	0.18
Pd_{org}/HCa	523	113	38	0.62
Pd_{aq}/HP	690	104	16	0.05
Pd_{org}/HP	645	115	27	0.09

[a] Temperature at 15% of CH_4 conversion.
[b] Activation energy calculated at methane conversion <20%.
[c] Experimental methane conversion at 700 °C.
[d] Experimental activity measured at 600 °C ($A_{600} = (X_{600}\,(\%) Q_{CH_4}\,(L\,s^{-1})/24.2\,(L\,mol^{-1}) \times 100) \times 10^{-6}$).

The calculated apparent activation energies (Table 3) remain almost constant around 100–114 kJ mol^{-1} whatever the nature of the precursor and the support synthesis conditions, suggesting that the same methane oxidation mechanism occurs on all the samples. Only slightly higher activation energy was obtained for the Pd/REF sample (148 kJ mol^{-1}). Corresponding Arrhenius plots are presented in Fig. 1B. Nevertheless, alumina is an almost inert support for the methane oxidation reaction in comparison with the transition metal-doped hexaaluminate supports that can explain why a slightly higher activation energy is obtained over the Pd/REF sample. These differences in term of activation energies were already observed

by Jang et al. [23] who reported activation energies between 62 kJ mol^{-1} and 65 kJ mol^{-1} over 2 wt% Pd/hexaaluminate whereas activation energy of 106 kJ mol^{-1} was obtained over 2 wt% Pd/Al_2O_3. Nevertheless, the addition of inhibitors in the feed (CO_2 and H_2O) can explain why slightly higher activation energies are obtained in our work. Some diffusional resistance over the hexaaluminate-based samples, cannot be excluded to explain the difference in activation energy between the two kinds of samples.

In conclusion, the activities measured over the different samples are mainly related to the palladium dispersion and the nature of the palladium precursor inducing various dispersions.

3.3. Thermal stability

Long-term catalyst stability was evaluated during 12 h under reaction at 700 °C. Results of the stability test are presented Fig. 3. Previous studies [6,15] showed that pure hexaaluminate samples (i.e. without palladium) presented excellent thermal stability at the temperature of reaction, comparison with those obtained for perovskite-type mixed oxides and conventional noble metal catalysts.

The reference sample Pd/REF which showed the highest initial activity, presented an almost linear deactivation under reaction (progressive decrease in methane conversion with reaction time, Fig. 3). Then, the conversion decreased from 95% at the beginning of the test to 61% after 12 h of reaction. This curve shape can stem from catalyst deactivation. The deactivation of Pd/Al_2O_3 catalyst was often reported in the literature [6,10] and is generally attributed to two main parameters: the thermal decomposition of the PdOx species at high reaction temperature [25,26] into less active Pd^0 phase; noble metal and/or support sintering [3,27]. Moreover, palladium catalysts deactivation is reported to occur even at low temperature (typically <500 °C), as clearly observed by Persson et al. [10]. In this work, methane conversion curve of the Pd/REF catalyst (Fig. 1A) shows two different trends. At temperature lower than 500 °C, methane conversion increases rapidly following a S-shape profile typical of the methane oxidation over this kind of solids. For temperatures higher than 500 °C, an almost linear increase in methane conversion is observed with the temperature, temperature similar to those reported by Persson et al. [10] for the beginning of the palladium active site deactivation. This lets us to suppose that the slowest linear increase in methane conversion for temperature higher than 500 °C originates from palladium deactivation, more than from diffusion limitations under reaction. Nevertheless, the in-situ XRD experiments performed by Persson et al. [10] did not show any bulk PdO decomposition up to 800 °C. However, the authors performed analysis under air, without methane in the feed.

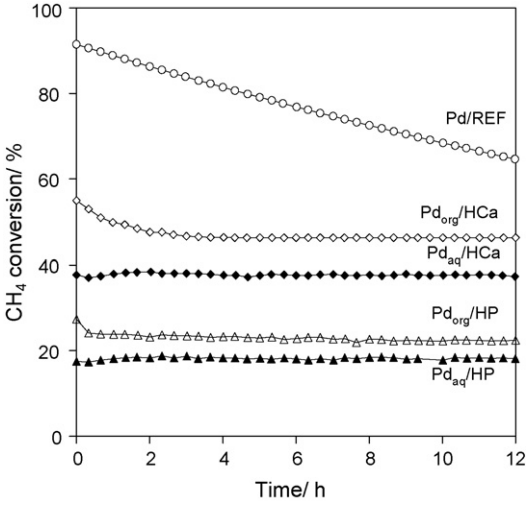

Fig. 3. Stability under reaction obtained for the different samples.

The results obtained in the study of the methane conversion stability as a function of time-on-stream (Fig. 3) over the palladium supported hexaaluminate catalysts strongly differ from those obtained over the reference sample. Two different trends are observed for these catalysts. Whereas the Pd_{aq} samples (Pd_{aq}/HCa and Pd_{aq}/HP, Fig. 3) present stable conversion along the 12 h under reaction, the two other samples prepared using palladium bis-acetylacetonate showed a fast decrease of the methane conversion during the first hour under reaction. The decrease in methane conversion is clearly observed for the Pd_{org}/HCa sample for which the conversion decreases from 55% to 49% after 2 h under reaction. Deactivation is less marked for the Pd_{org}/HP sample. At the end of the test, the difference in term of catalytic activity between samples prepared from organic impregnation route or aqueous impregnation route, remains rather low (Fig. 3).

4. Mechanism of deactivation

As already mentioned, deactivation can stem from different parameters: palladium active site reduction under reaction; palladium and/or support sintering. On the basis of the results obtained for the catalysts prepared using palladium nitrate, as palladium source, it can be concluded that the support does not suffer from sintering or deactivation under the test conditions (Fig. 3). Then, the two parameters that can be the source of catalyst deactivation are: palladium oxidized site reduction and palladium particle sintering.

In order to discriminate the role of each parameter on the measured deactivation, reduction–reoxidation cycles were performed at the end of the first temperature increase ramp on three samples (Fig. 4): Pd/REF, Pd_{aq}/HCa and Pd_{org}/HCa. The reduction–reoxidation cycles consist in three successive steps:

1. Reduction under 4% H_2/N_2 at 700 °C followed by reaction under the same conditions than for the catalytic test.
2. Reduction under 4% H_2/N_2 at 700 °C and reoxidation under 10% O_2/N_2 at 700 °C followed by reaction under the same conditions than for the catalytic test.
3. Reduction under 4% H_2/N_2 at 700 °C and reoxidation under 10% O_2/N_2 at 500 °C followed by reactant gas mixture $N_2/O_2/CO_2/H_2O/CH_4$.

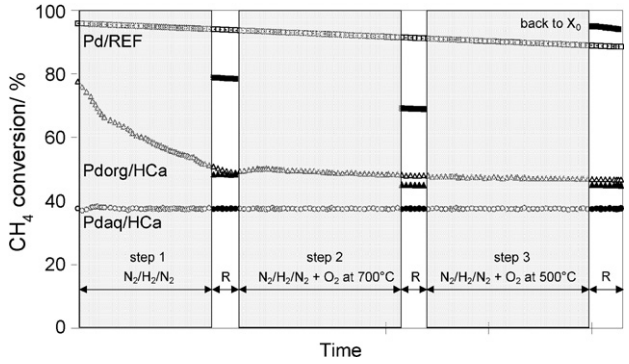

Fig. 4. Stability of Pd/REF and Pd-supported HCa samples under reduction–oxidation treatment. Grey, reduction–oxidation cycles; *R*, reaction under oxidation test mixture (N_2/O_2/4 vol% CO_2/4 vol% H_2O/1 vol% CH_4); open symbols, conversion measured during stability test.

This procedure was preferred to conventional reduction–reoxidation procedure obtained under dynamic conditions (temperature programmed reduction, temperature programmed oxidation) since each reduction–oxidation cycle is performed under isothermal conditions that allows one to measure the catalytic activity of the sample after each cycle. Results are shown Fig. 4 and compared with the methane conversion evolution during the stability test after the first light-off at the same time under reaction (open symbols).

For the Pd/REF sample, a reducing step (step 1) under 4% H_2 at 700 °C leads to a decrease of the catalytic activity. A methane conversion of 79% is then obtained that is largely lower than that obtained without reducing treatment (94%). A further reduction cycle at 700 °C followed by a reoxidation step under O_2 at 700 °C (step 2) leads to a supplementary loss in catalytic activity, with a methane conversion at the end of this step of 69% (92% without step 2). Nevertheless, it was observed that a third reduction cycle with subsequent oxidation at 500 °C (step 3) leads to a 95% conversion, i.e. to the initial activity of the Pd/REF sample. It is observed that the methane conversion decrease starts at a similar rate as for the sample without any reduction–reoxidation cycles. The results obtained during these experiments let us conclude to a reversible deactivation mechanism under the test conditions. This behaviour suggests that Pd/REF deactivation is not due to sintering of PdOx particles but is only due to progressive reduction of the PdOx active phase into less active metallic Pd. Indeed, Pd particle redispersion is effective only under drastic oxychlorination treatments [28]. Then, results showed that Pd^0 reoxidation (and consequently activity recovering) occurs after reoxidation at 500 °C, and it is not possible to reoxidize reduced palladium sites under oxidative treatment at 700 °C.

The same experiment performed over the HCa support (without palladium) showed that the hexaaluminate structure is not sensitive to this kind of reducing treatment [15]. The effect of reduction–reoxidation cycles was studied over Pd_{aq}/HCa (Fig. 4). It is clearly observed that the so-performed experiment has no effect on the methane conversion over the Pd_{aq}/HCa sample that remains constant at 38% during all the 12 h of the test. Since it was previously observed that the palladium phases present on the surface of this catalyst are PdO and PdO_2 [15], it can be concluded that hexaaluminate compounds are efficient supports for the stabilization of the palladium in its oxidized form, even under reaction at temperature as high as 700 °C.

By contrast, stability results obtained for the Pd_{org}/HCa sample after the first light-off curve show drastic deactivation of the catalyst under the test conditions (Fig. 4). Whereas an initial conversion of 78% is obtained at the end of the first temperature ramp (Fig. 2, open diamond; beginning of the stability test, Fig. 4), conversion decreases up to 50% (after only 2 h, Fig. 4). It is observed that the first reduction cycle (step 1) leads to a decrease of the methane conversion over Pd_{org}/HCa (Fig. 4) that stabilizes around 48%. Nevertheless, this conversion is close to that obtained during simple stability test (open symbol, Fig. 4). A further reduction–reoxidation at 700 °C cycle (step 2) leads to minor change in the methane conversion that decreases up to 45%. Then, as already observed for the Pd/REF samples, no beneficial effect of a reoxidation step at 700 °C on the catalyst activity can be observed. Similarly, the third step (reduction, followed by reoxidation at 500 °C) does not result in any change in methane conversion that remains constant around 45%. This strongly differs from the results obtained over the Pd/REF sample for which a return to the initial activity is observed after step 3. As a consequence, deactivation observed over Pd_{org}/HCa cannot be related to a reversible PdOx site reduction, and might be attributed to the sintering of palladium particles during reaction. Unfortunately, it was not possible to perform palladium dispersion measurement over this catalyst after test since the weight sample is too low. Only TEM analysis was performed before and after catalytic test. Before test, palladium particle sizes are smaller than 5 nm (Fig. 5A and C). After test, a visible growth of particles is observed, with sizes largely higher than 5 nm (Fig. 5B and D). Even if a quantification of the palladium particle growth is not possible from the TEM pictures, the sintering is however clearly suggested by the TEM micrographs (compare Fig. 5C and D). This deactivation mechanism is however not reversible since palladium particle redispersion can be only observed under specific conditions like drastic oxychlorination treatments. In conclusion, palladium particles obtained from organic impregnation route seems to present lower stability than those obtained from aqueous impregnation route. Lesage-Rosenberg et al. [22] however observed that the anchorage of the active Pd^{2+} cation on the carrier involved octahedral aluminium vacant sites, giving locally a phase close to an aluminate. But this phase is unstable, and the topology of the carrier surface is supposed to play an important role on the final state of Pd dispersion. For $Pt(acac)_2$ precursor, Womes et al. [29] observed different kinds of adsorption site onto alumina surface. Sites are formed after partial dehydroxylation of the surface at temperatures up to 350 °C, one of low reactivity (type A) on which is anchored by simple physisorption, and one of high reactivity (type B). Precursor adsorption induces partial decomposition of the complex where the remaining Pt–acac is chemically bonded to surface oxygen atoms. It can be logically proposed that the chemisorbed PdOx particles located on sites similar to those of type A for $Pt(acac)_2$ precursor can suffer from sintering under

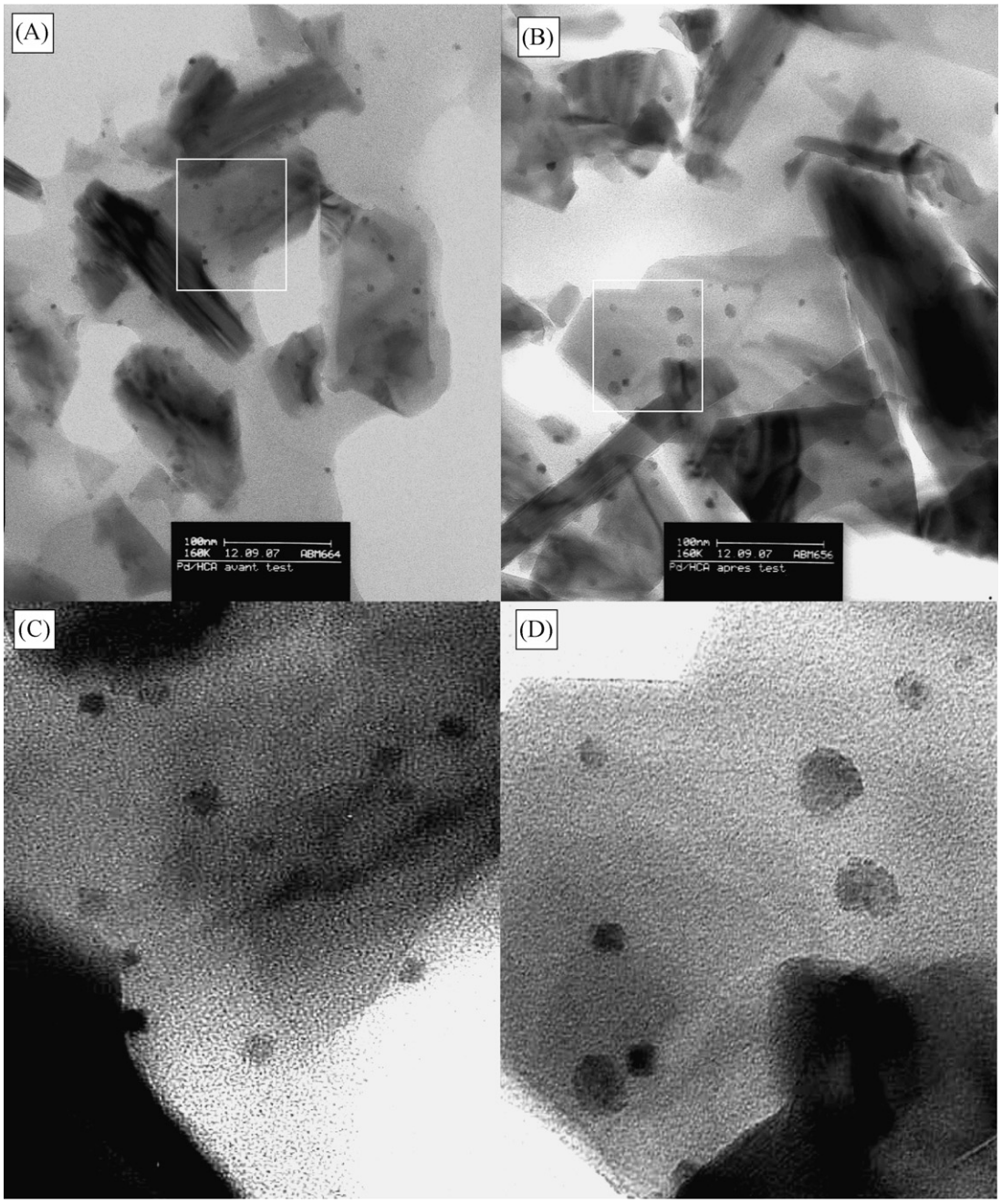

Fig. 5. TEM pictures obtained for Pd_{org}/HCa before (A) and (C) and after catalytic tests (B) and (D). Pictures (C) and (D) are the magnifications of the squares in figures (A) and (B).

reaction, because of the weak interaction between the adsorption site and the palladium precursor. Then, stabilization of the palladium particles to a size near of that obtained for catalysts prepared using the aqueous route allows to explain why similar activity is obtained after stabilization whatever the nature of the palladium precursor.

5. Conclusion

We reported here the effect of the palladium precursor salt on the catalytic activity and stability under reaction for a series of Pd-supported hexaaluminate samples. It was observed that the samples prepared using $Pd(acac)_2$ as palladium source present higher palladium dispersion (i.e. smaller crystal sizes), and consequently higher catalytic activity for the methane oxidation reaction. Nevertheless, these samples quickly deactivate under reaction, and stabilize at a methane conversion close to those obtained over samples prepared using palladium nitrate as precursor. Contrarily to what was observed on the reference Pd/Al_2O_3 sample, deactivation is not reversible under reoxidizing treatment, suggesting a sintering of the small Pd particle into larger one. This sintering of palladium particle can be logically related to the nature of $Pd(acac)_2$ adsorption sites. Weak interaction between the organic precursor and the support

allow a further sintering of particles during reaction that was not observed over samples synthesized using $Pd(NO_3)_2$ salt precursor. After stabilization, samples present similar catalytic activity whatever the palladium precursor used.

Acknowledgements

The French "Agence de l'Environnement et de la Maîtrise de l'Energie" (ADEME) and RENAULT SAS are warmly acknowledged for financial support.

References

[1] M.F.M. Zwinkels, S.G. Jaras, P.G. Menon, T.A. Griffin, Catal. Rev. Sci. Eng. 35 (1993) 319.
[2] J.G. McCarty, Nature 403 (2000) 35.
[3] T.V. Choudhary, S. Banerjee, V.R. Choudhary, Appl. Catal. A 234 (2002) 1.
[4] P. Courty, H. Ajot, C. Marcilly, B. Delmon, Powder Technol. 7 (1973) 21.
[5] G. Groppi, C. Cristiani, P. Fortzatti, Appl. Catal. B 35 (2001) 137.
[6] S. Royer, C. Ayrault, C. Carnevillier, F. Epron, P. Marécot, D. Duprez, Catal. Today 117 (2006) 543.
[7] D. Ciuparu, M.R. Lyubosky, E. Altman, L.D. Pfefferle, A. Datye, Catal. Rev. 44 (2002) 593.
[8] Y. Ozawa, Y. Tochihara, A. Watanabe, M. Nagai, S. Omi, Appl. Catal. A 259 (2004) 1.
[9] H. Arai, H. Fuzukawa, Catal. Today 26 (1995) 217.
[10] K. Persson, A. Ersson, S. Colussi, A. Tovarelli, S.G. Jaras, Appl. Catal. B 66 (2006) 175.
[11] L.S. Escandon, S. Ordonez, A. Vega, F.V. Diez, Chemosphere 58 (2005) 9.
[12] G. Groppi, M. Bellotto, C. Cristiani, P. Forzatti, P.L. Villa, Appl. Catal. A 104 (1993) 101.
[13] M. Bellotto, G. Artioli, C. Cristiani, P. Forzatti, G. Groppi, J. Catal. 179 (1998) 597.
[14] L. Lietti, C. Cristiani, G. Groppi, P. Forzatti, Catal. Today 59 (2000) 191.
[15] A. Baylet, S. Royer, P. Marécot, J.M. Tatibouet, D. Duprez, Appl. Catal. B 77 (2007) 237.
[16] L.M.T. Simplicio, S.T. Brandao, E.A. Sales, L. Lietti, F. Bozon-Verduraz, Appl. Catal. B 63 (2006) 9.
[17] D. Roth, P. Gélin, A. Kaddouri, E. Garbowski, M. Primet, E. Tena, Catal. Today 112 (2006) 134.
[18] K. Persson, P.O. Thevenin, K. Jansson, J. Agrell, S.G. Jaras, L.J. Pettersson, Appl. Catal. A 249 (2003) 165.
[19] D. Duprez, J. Chim. Phys. 80 (1983) 487.
[20] F. Klingstedt, H. Karhu, A. Kalantar Neyestanaki, L.-E. Lindfors, T. Salmi, J. Väyrynen, J. Catal. 206 (2002) 248.
[21] R.S. Monteiro, L.C. Dieguez, M. Schmal, Catal. Today 65 (2001) 77.
[22] E. Lesage-Rosenberg, G. Vlaic, H. Dexpert, P. Lagarde, E. Freund, Appl. Catal. 22 (1986) 211.
[23] B.W.-L. Jang, R.M. Nelson, J.J. Spivey, M. Ocal, R. Oukaci, G. Marcelin, Catal. Today 47 (1999) 103.
[24] K. Sekizawa, K. Eguchi, H. Widjaja, M. Machida, H. Arai, Catal. Today 28 (1996) 245.
[25] R. Strobel, S.E. Pratsinis, A. Baiker, J. Mater. Chem. 15 (2005) 605.
[26] M. Peuckert, J. Phys. Chem. 89 (1985) 2481.
[27] R. Burch, F.J. Urbano, Appl. Catal. A 124 (1995) 121.
[28] J.A. Anderson, R.A. Daley, S.Y. Christou, A.M. Efstathiou, Appl. Catal. B 64 (2006) 189.
[29] M. Womes, T. Cholley, F. Le Peltier, S. Morin, B. Didillon, N. Szydlowski-Schildknecht, Appl. Catal. A 283 (2005) 9.